

Mechanism of 2'-fucosyllactose degradation by human-associated *Akkermansia*

Loren Padilla,¹ Ashwana D. Fricker,¹ Estefani Luna,¹ Biswa Choudhury,² Elizabeth R. Hughes,³ Maria E. Panzetta,³ Raphael H. Valdivia,³ Gilberto E. Flores¹

AUTHOR AFFILIATIONS See affiliation list on p. 15.

ABSTRACT Among the first microorganisms to colonize the human gut of breastfed infants are bacteria capable of fermenting human milk oligosaccharides (HMOs). One of the most abundant HMOs, 2'-fucosyllactose (2'-FL), may specifically drive bacterial colonization of the intestine. Recently, differential growth has been observed across multiple species of *Akkermansia* on various HMOs including 2'-FL. In culture, we found growth of two species, *A. muciniphila* Muc^T and *A. biwaensis* CSUN-19, on HMOs corresponded to a decrease in the levels of 2'-FL and an increase in lactose, indicating that the first step in 2'-FL catabolism is the cleavage of fucose. Using phylogenetic analysis and transcriptional profiling, we found that the number and expression of fucosidase genes from two glycoside hydrolase (GH) families, GH29 and GH95, vary between these two species. During the mid-log phase of growth, the expression of several GH29 genes was increased by 2'-FL in both species, whereas the GH95 genes were induced only in *A. muciniphila*. We further show that one putative fucosidase and a β -galactosidase from *A. biwaensis* are involved in the breakdown of 2'-FL. Our findings indicate that the plasticity of GHs of human-associated *Akkermansia* sp. enables access to additional growth substrates present in HMOs, including 2'-FL. Our work highlights the potential for *Akkermansia* to influence the development of the gut microbiota early in life and expands the known metabolic capabilities of this important human symbiont.

IMPORTANCE *Akkermansia* are mucin-degrading specialists widely distributed in the human population. *Akkermansia biwaensis* has recently been observed to have enhanced growth relative to other human-associated *Akkermansia* on multiple human milk oligosaccharides (HMOs). However, the mechanisms for enhanced growth are not understood. Here, we characterized the phylogenetic diversity and function of select genes involved in the growth of *A. biwaensis* on 2'-fucosyllactose (2'-FL), a dominant HMO. Specifically, we demonstrate that two genes in a genomic locus, a putative β -galactosidase and α -fucosidase, are likely responsible for the enhanced growth on 2'-FL. The functional characterization of *A. biwaensis* growth on 2'-FL delineates the significance of a single genomic locus that may facilitate enhanced colonization and functional activity of select *Akkermansia* early in life.

KEYWORDS *Akkermansia*, HMOs, 2'-FL, transcriptomics, glycoside hydrolase

The foundation of the human gut microbiome begins at birth and is shaped by the initial diet of the newborn, namely human milk (1). Human milk is 87%–88% water with a solid fraction made up of carbohydrates (7%), lipids (3.8%), proteins (1%), and other bioactive compounds including hormones and antibodies (2–4). Carbohydrates include lactose and a diversity of other bioactive sugars called human milk oligosaccharides (HMOs) (5). HMOs are the third most abundant component of human milk yet are indigestible by human enzymes (6, 7), and therefore reach the large intestine largely

Editor Laurie E. Comstock, University of Chicago, Chicago, Illinois, USA

Address correspondence to Ashwana D. Fricker, ashwana.fricker@csun.edu, or Gilberto E. Flores, gilberto.flores@csun.edu.

Loren Padilla and Ashwana D. Fricker contributed equally to this article. Order was chosen by agreement between co-authors.

Raphael Valdivia is a co-founder of Bloom Sciences (San Diego, CA).

See the funding table on p. 15.

Received 14 October 2023

Accepted 4 January 2024

Published 1 February 2024

Copyright © 2024 Padilla et al. This is an open-access article distributed under the terms of the [Creative Commons Attribution 4.0 International license](https://creativecommons.org/licenses/by/4.0/).

intact where they act as prebiotics for early bacterial colonizers of the human gut (8). HMOs are composed of only five monosaccharide units (glucose, galactose, N-acetylglucosamine, fucose, and N-acetylneuraminic acid) that form structurally complex linear and branched polysaccharides (9–11). The presence and concentration of these HMOs vary across individuals and are influenced by maternal genetics (12, 13). For example, one of the HMOs, 2'-FL, is highly produced by mothers with an active *FUT2* secretor gene, accounting for ~30% of the total HMOs in these individuals (5). Higher levels of 2'-FL correlate with lower levels of allergies, and lower incidence of eczema and diarrhea in infants (14). In addition to regulating the host immune system, bacterial fermentation of HMOs produces short-chain fatty acids (SCFA) that help maintain the intestinal epithelium and regulate appetite (15).

While only a few microorganisms in the infant's gut possess the ability to use the entire suite of HMOs, many are capable of fermenting components of HMOs for growth (16–18). For instance, *Bifidobacteria* encode both glycoside hydrolases (GH) and transport systems (19, 20) to catabolize HMOs. However, there are species and strain-to-strain variability in the mechanisms for HMO degradation across *Bifidobacteria*. For example, *Bifidobacterium longum* subsp. *infantis* uses intracellular enzymes, whereas *Bifidobacterium bifidum* uses extracellular enzymes, pointing to differences in competitive strategies between these organisms (19–22). In addition, other intestinal bacteria such as *Bacteroides thetaiotaomicron* and *Bacteroides fragilis* repurpose machinery primarily responsible for the breakdown of mucins to degrade HMOs (23).

The genus *Akkermansia* is comprised of commensal mucin-degrading bacteria that colonize the gastrointestinal tract from early life to adulthood (24) and can also use HMOs for growth (25–27). During growth on HMOs, *Akkermansia* produces acetate, succinate, and propionate (26). The most abundantly produced SCFA, acetate, is involved in fueling gastrointestinal epithelial cells, leading to mucin secretion, and helping to maintain gut barrier integrity (28). In infant guts, there is a positive correlation between the abundance of *Akkermansia* and fucosylated HMOs in the mother's breast milk (29, 30), suggesting a role for this organism in HMO metabolism *in vivo*. Given that *Akkermansia* are largely considered beneficial members of the gut microbiome (31), understanding their ability to degrade HMOs may lead to therapeutic applications.

Although *Akkermansia* are predominantly mucin-degrading specialists, given the structural and compositional similarities between HMOs and mucin oligosaccharides, species may use similar enzymes to break down HMOs (26, 32). Most of the efforts in developing a mechanistic understanding of *Akkermansia* utilization of host glycans thus far have centered around a single isolate of *A. muciniphila* (Muc^T). The Muc^T strain has been shown to use a diversity of GHs including fucosidases, β -hexosaminidases, and β -galactosidases for degrading a variety of human glycans including HMOs and lactose (26, 32, 33). Recently, we and others have identified and isolated at least four species-level phylogroups (Aml–AmlV) of human-associated *Akkermansia*. Thus far, three phylogroups have been named, *A. muciniphila* (Aml), *A. massiliensis* [AmlI (34)], and *A. biwaensis* [AmlV (35)]. The fourth phylogroup, AmlIII, is represented by our CSUN-56 isolate and two isolates from Guo and colleagues (36) but is not yet formally named.

We recently demonstrated that all four of these human-associated *Akkermansia* species have the genetic potential and functional ability to metabolize and grow using a variety of HMOs (27). Moreover, some species were more efficient and grew better on individual HMOs. In particular, *A. biwaensis* strain CSUN-19 (AmlV), grew to higher final optical densities (OD) on a suite of HMOs and encodes for a larger complement of putative GHs associated with HMO degradation. Interestingly, despite high growth yields when grown on 2'-FL, *A. biwaensis* consumed the least amount of the HMO across *Akkermansia* species. We hypothesized that strains with a greater ability to grow on 2'-FL will have greater expression of GHs or additional GHs required for growth on this substrate. Through phylogenetic analysis, transcriptional profiling, and heterologous expression systems, we identified genes encoding putative fucosidases (GH29 and GH95) and a β -galactosidase (GH2) from *A. biwaensis* involved in 2'-FL degradation.

MATERIALS AND METHODS

Phylogenetic analysis of putative fucosidase encoding genes

To determine the phylogenetic relationships of select glycoside hydrolase (GH) genes across *Akkermansia* species, we analyzed the genomes of 17 publicly available isolates spanning the known phylogenetic diversity of human-associated *Akkermansia* (36–39). Genome accession numbers of isolates used in the analysis are provided in Table S1 (Table S1). Assembled genomes were submitted to the dbCAN meta server for annotation of GH encoding genes (40, 41). dbCAN uses several tools for annotation and we considered only annotations that agreed using HMMER (42) and DIAMOND (43). All genes annotated as GH2, GH29, and GH95 were identified in the dbCAN output, extracted from the genomes of each strain, imported into MEGA11 (44–46), and aligned using MUSCLE (47, 48). Maximum likelihood trees for each GH family were generated in MEGA11 using default parameters with 100 bootstrap iterations. After the identification of putative fucosidases involved in 2'-FL catabolism, GH29 gene annotations from *A. muciniphila* Muc^T, and *A. biwaensis* CSUN-19 were phylogenetically compared to functionally characterized GH29 fucosidases from other intestinal bacteria (49–54). Accession numbers for proteins and the associated organisms used in the analysis are provided in Table S2 (Table S2). For these analyses, amino acid sequences were aligned using MUSCLE, and a maximum likelihood tree was generated in MEGA11 using default parameters with 50 bootstrap iterations.

Growth on fucosylated HMOs

Previously, we showed growth of diverse *Akkermansia* on 2'-FL in medium with 0.5% mucin (27). Since mucin also contains fucose residues with the same α -1,2 configuration as 2'-FL, we first determined the growth of *A. muciniphila* Muc^T ATCC BAA-835 (AmI) and *A. biwaensis* CSUN-19 (AmIV) on 2'-FL in the absence of mucin in basal tryptone threonine medium (BTTM) previously described by Ottman and colleagues (25). Briefly, this medium contains 3 mM KH₂PO₄, 3.5 mM Na₂HPO₄, 5 mM NaCl, 0.5 mM MgCl₂·6H₂O, 47.6 mM NaHCO₃, 0.7 mM CaCl₂·2H₂O, 5.6 mM NH₄Cl, 18 g/L Tryptone (Oxoid, USA), 1.3 g/L L-Threonine, 0.05% Na₂S·9H₂O, 1× trace mineral solution (55), and ATCC vitamins (final 1% vol/vol, manufacturer's number: ATCC MD-VS, Hampton, NH) with an anaerobic headspace of 70% N₂ and 30% CO₂. Stock cultures were maintained in 5 mL BTTM containing 0.4% vol/vol soluble type III porcine gastric mucin prepared as described previously (27, 55). Mucin in these cultures provides both carbon and a source of N-acetylglucosamine (GlcNAc), for which *Akkermansia* is auxotrophic (56). To obtain mucin-free bacterial cultures, organisms were sub-cultured at 10% inoculum in 5 mL BTTM to which 0.25 mL of 200 mM GlcNA and 0.125 mL of 200 mM glucose (Glc) was added. Subsequently, for RNAseq, a 10% inoculum was transferred to 10 mL BTTM with the addition of 0.5 mL 200 mM GlcNAc and 0.25 mL of either 200 mM Glc or 200 mM 2'-FL (Glycom, Hørsholm, Denmark). The estimated final concentrations of sugars are 8.3 mM GlcNAc, 4.15 mM Glc, and 4.15 mM 2'-FL. Prior to inoculation, each sugar or mucin was filter sterilized (UNIFLO 13 mm 0.2 μ M PES Filter Media, Whatman) and added to the media.

All cultures were incubated at 37°C in a Vinyl Anaerobic Chamber (Coy Laboratory Products, Incorporated, Grass Lake, MI). To monitor growth, 500 μ L of each culture was used to determine OD_{600nm} on a Biophotometer plus spectrophotometer (Eppendorf, Biophotometer Plus). Cultures with an OD_{600nm} > 1.0 were diluted with sterile BTTM and re-read. All experimental cultures were grown in quadruplicate.

For follow-up growth experiments with the Akk-EH114 (Muc^T Tn-*Amuc_2072::HHJ01_10880*—see below) strain, the following sugar concentrations were used: 4 mM 2'-FL (Glycom, Hørsholm, Denmark) with 0.4% porcine mucin. *Akkermansia* was grown overnight in 5 mL basal mucin medium (27) with 0.4% porcine mucin, sub-cultured in 1 mL BTTM containing media with the appropriate sugars, and 200 μ L was transferred to a flat clear-bottom 96-well plate and read hourly on a Spectrostar

Nano plate reader (BMG Labtech, USA) for 46 ± 2 hours with 37°C incubation and 10 seconds of orbital shaking prior to each read. Optical density was converted to $\text{OD}_{600\text{nm}}$ using a linear equation and the initial ($t = 0$) read was subtracted from all time points as a media blank. All cultures were grown in triplicate and each experiment was repeated three times, except where indicated.

Statistically significant differences between growth at 24 hours were calculated by Tukey's honest significance multiple comparisons test using R 4.1.1 (R Foundation for Statistical Computing, Vienna, Austria). Comparisons were considered significant if corrected P -values were less than 0.05. Symbol style for figures: nonsignificant (ns), 0.05 (*), 0.01 (**), 0.001 (***) and <0.0001 (****).

Targeted metabolomics

Culture supernatants were collected to measure 2'-FL and Glc degradation during RNA harvest time points. In addition to each parent sugar (2'-FL, Glc, and GlcNAc), their sugars (fucose, lactose, glucose, and galactose) were also quantitatively measured using high-performance anion exchange chromatography with pulsed amperometric detection (HPAEC-PAD) (57). Culture supernatants were transported frozen (dry ice) where they were thawed in a water bath, vortexed to homogenize, and centrifuged at $7,000 \times g$ for 5 minutes at 10°C . Then, $0.5 \mu\text{L}$ of the culture media was injected into the HPAEC-PAD for the detection of the expected analytes described above. Carbohydrate analyses were done as described previously (27).

RNA extraction and purification

RNASeq was performed on cultures grown in BTTM supplemented with GlcNAc and either Glc or 2'-FL (described above) to identify potential genes involved in 2'-FL degradation. Samples were collected at approximately mid-log growth for each condition/species combination. For *A. muciniphila* Muc^T, samples were collected after 12 hours of growth on Glc and 49 hours for growth on 2'-FL. For *A. biwaensis* CSUN-19, samples were collected after 14 hours of growth on Glc and 34 hours of growth on 2'-FL. At the indicated time points, 1 mL of each culture was centrifuged for 7 minutes at 4°C and $10,000 \times g$. Supernatants from each pelleted sample were removed and placed in the -80°C freezer for metabolomics analysis and pellets were flash frozen in liquid nitrogen before storage at -80°C . RNA was extracted from cell pellets using the phenol/chloroform extraction method outlined in the protocol in RiboPure Bacteria Kit (Life Technologies Corporation, Carlsbad, CA). Molecular grade Chloroform (MP Biomedicals, LLC, Solon, OH) and Absolute Ethanol (200 proof) (Fisher Bioreagents, Fisher Scientific, Fair Lawn, NJ) were used for the chloroform/ethanol steps. The elution solution was replaced by water (for RNA work) that is nuclease-free and DEPC-treated (Fisher Bioreagents, Fisher Scientific, Fair Lawn, NJ). A total of $50 \mu\text{L}$ was eluted in two steps ($25 \mu\text{L}$ each step) with 10-minute incubations for each elution step. Two DNase treatments were completed of 1-hour duration each: DNase I treatment from the RiboPure Bacteria Kit followed by Turbo DNase treatment (Life Technologies Corporation, Carlsbad, CA). During Turbo DNase treatment, a master mix containing $5 \mu\text{L}$ turbo DNase buffer and $1 \mu\text{L}$ turbo DNase per sample was made prior to adding to the samples. The reagent used for the Turbo DNase inactivation was the same as the RiboPure Bacteria Kit.

RNA was purified and concentrated according to the protocol for RNA Clean and Concentrator Kit - 5 (Zymo Research Corporation, Irvine, CA) with an eluted volume between 30 and $35 \mu\text{L}$. Final RNA concentrations were measured using the Qubit 2.0 Fluorometer with RNA High Sensitivity (HS) Assay Kit (Life Technologies Corporation, Carlsbad, CA) after the purification. All samples were stored at -20°C until submission to Novogene USA, Inc. for Total RNA Sequencing.

RNA sequencing and analysis

RNA samples were sequenced by Novogene USA, Inc. using the Illumina Sequencing HiSeq platform (Illumina, CA, USA). Quality control of RNA samples was assessed using

High Sensitivity RNA ScreenTape on TapeStation (Agilent Technologies Inc., CA, USA) and quantified using the Qubit 2.0 RNA High Sensitivity assay (ThermoFisher, MA, USA). Ribosomal RNA depletion was performed with Ribo-Zero Plus rRNA Removal Kit (Illumina Inc., CA, USA). Samples were primed and fragmented based on the recommendation of the manufacturer. First-strand synthesis was performed with Protoscript II Reverse Transcriptase using a longer extension step of ~30 minutes at 42°C. NEBNext UltraTM II Non-Directional RNA Library Prep Kit for Illumina (New England BioLabs Inc., MA, USA) was used for the remaining steps of library construction. The final library size was around 350 bp with an insert size of 200 bp. The final quantity of the library was quantified using Qubit 2.0 and the quality was assessed by the TapeStation D1000 ScreenTape (Agilent Technologies Inc., CA, USA). For the Illumina HiSeq, 8-nt dual-indices were used and equimolar pooling of libraries was done based on the values from the QC before sequencing with a read length configuration of 150 PE for 20 M PE reads per sample (20M in each direction).

RNA sequencing analysis was performed using the DIY.transcriptomics pipeline (<https://diytranscriptomics.com>) (58). Raw reads from transcriptomic data were mapped to coding sequences (CDs, no rRNA, or tRNA) of each strain using Kallisto (59). The remaining analyses were completed in Rstudio (<https://www.rstudio.com>) (File S1 and S2). Kallisto transcript abundance measurements were imported into RStudio using the R package *tximport* (60) for filtering and normalization. The Bioconductor/R package *edgeR* (61) *cpm* function was used to create a list of counts per million (cpm) per transcript. Genes with no cpm were filtered out of the data set using base R's subsetting method. The *edgeR* function *calcNormFactors* was used to normalize the filtered data using the TMM method (Trimmed Mean of M-values) to the data set (62).

For analyses of differentially expressed genes (DEGs), a design matrix targeting treatment (Glc versus 2'-FL) was set up to compare the cpm of genes in the Glc control versus the 2'-FL treatment. To create a model mean-variance trend and fit the linear model to the data, the *voom* function from the Bioconductor/R package *limma* (63) was used to model a mean-variance relationship, the function *lmfit* was used to fit a linear model to the data, and *makeContrasts* was used to make contrasts of the design matrix between the 2'-FL group versus the Glc group. Bayesian statistics were computed for the linear model fit using the *eBayes* function from *limma* which resulted in moderated statistical values of differential expression (Adjusted *P*-value, Log fold change, Average Expression, T statistics). To extract DEGs from the linear model fit and Bayesian analysis, the function *decideTests* from *limma* was used to generate a list of significantly regulated DEGs with strict cutoff values (corrected *P* value ≤ 0.01 , log₂ fold change ≥ 2) (64).

The R package *EnhancedVolcano* was used to generate volcano plots highlighting the GH29 and GH95 genes for each *Akkermansia* strain with strict cutoff values ($P_{adj} \leq 0.05$, log₂ fold change ≥ 2) (65).

Cloning and purification of putative β -galactosidase in *E. coli*

To characterize one of the β -galactosidases that may be involved in 2'-FL metabolism, the gene fragment of the HHJ01_10865 protein, which encodes the mature GH2 protein lacking the signal peptide (as predicted by SignalP 5.0) (66) was amplified from *A. biwaensis* CSUN-19 genomic DNA using the primers as shown in Table S3 (Table S3), cut with *HindIII* and *EcoRI* and inserted into the expression vector pET28a(+) (Novagen, Inc.). The resulting recombinant plasmids were transformed into *E. coli* Tuner BL21 for protein overexpression. Bacterial cultures were grown in 50 mL LB medium with kanamycin (50 μ g/mL) at 37°C to OD_{600nm} ~ 0.5, followed by induction with 1 mM isopropyl β -D-1-thiogalactopyranoside (IPTG) for 2 hours at 37°C. Cells were harvested by centrifugation (5,000 $\times g$ for 5 minutes at 4°C), and the cell pellets were flash-frozen in liquid nitrogen for 5 minutes and stored at -20°C until purification.

Thawed cell pellets were resuspended in 5 mL of purification buffer (50 mM Tris pH 8.0, 200 mM NaCl) and lysed by 4 rounds of sonication (2 minutes of 1 second on/2 seconds off) with 40% amplitude (Qsonica, USA). Lysates were centrifuged for

30 minutes at $38,000 \times g$ and 4°C and cleared supernatants loaded onto Ni-NTA columns with 0.5 mL bed volume (1018244 Qiagen, Germany). The columns were washed sequentially with three column volumes (CV) each of the purification buffer, a low-imidazole wash, and a mid-imidazole wash. Bound proteins were eluted with 4 CV of 100 mM imidazole in a purification buffer. Fractions containing recombinant protein, as assessed by SDS-PAGE analysis, were combined and dialyzed against the purification buffer, and the final protein concentration was determined using the Qubit protein assay kit (#Q33211 Life Technologies Corporation, USA).

Activity of purified proteins

All enzyme activity and inhibition reactions were performed in 50 mM Tris, 200 mM NaCl, pH 8.0, unless otherwise indicated. Reactions involving 2.5 mM ONPG were carried out for 1 hour at 37°C . The enzymatic product of the analog, orthonitrophenol (ONP), was determined by measuring $A_{405\text{ nm}}$ using a 96-well plate reader Spectromax M5 (Molecular Devices, USA) and monitored every 5 minutes for 1 hour following the addition of substrate.

Expression of *A. biwaensis* HHJ01_10880 in *A. muciniphila* Muc^T

The gene encoding the putative *A. biwaensis* GH29 fucosidase HHJ01_10880 (clade 4) was introduced into *A. muciniphila* Muc^T using a modified mariner transposon (Tn) delivery system (pSAM_Akk) (67). The plasmid was re-engineered to insert genes within the inverted repeats of the Tn system and enable the expression of genes of interest in *A. muciniphila* under the control of the promoter of *Amuc_1505* (RNA pol) promoter. The resulting plasmid (pE_Akk) contains a *cat* resistance cassette and the *Amuc_1505* promoter flanked by *Mariner* transposase recognition sites.

The coding sequence of HHJ01_10880 was amplified by PCR from *A. biwaensis* Akk2750 (100% sequence match to CSUN-19) (38) with Q5 Hot Start High-Fidelity DNA Polymerase (New England Biolabs) and incorporating a C-terminal HA epitope tag. The amplicon was inserted into *Sall*- and *FseI*-digested pE-Akk via In-Fusion Snap Assembly (Takara Bio). The correct sequence of pE_Akk_10880 was confirmed by Nanopore sequencing (Plasmidsaurus).

pE_Akk_10880 was introduced into *E. coli* S17-1 λ pir strain for conjugative transfer into *A. muciniphila* Muc^T as outlined by Davey et al., with minor modifications (67). Briefly, the *E. coli* strain carrying pE_Akk_10880 and *A. muciniphila* Muc^T were co-incubated ~16 hours in a 10:1 under aerobic conditions on synthetic agar plates [3 mM KH_2PO_4 , 3 mM Na_2PO_4 , 5.6 mM NH_4Cl , 1 mM MgCl_2 , 1 mM $\text{Na}_2\text{S}_9\text{H}_2\text{O}$, 47 mM NaHCO_3 , 1 mM CaCl_2 , 40 mM HCl, trace elements and vitamins, 0.2% GlcNAc, 0.2% glucose, 16 g l⁻¹ soy peptone, 4 g l⁻¹ threonine, 1.25% agar (68, 69)] with 0.5 g l⁻¹ thioglycolate added and lacking the added sugars (GlcNAc and glucose). After conjugation, cells were diluted and transferred into a synthetic medium supplemented with 20 μM ciprofloxacin and grown anaerobically for 48 hours. Bacterial cells were passaged twice by diluting 1:10 into fresh medium for 24 hours, before spreading onto synthetic agar plates containing an additional 0.25% mucin with ciprofloxacin and chloramphenicol (7 $\mu\text{g}/\text{mL}$) and incubated at 37°C until colonies were large enough to pick (~6 days). Four chloramphenicol-resistant colonies were picked and Tn insert locations mapped by arbitrary PCR.

Expression of HHJ01_10880 was confirmed via western blot (Fig. S1). Samples were separated on a 12% SDS-PAGE gel and subsequently blotted on nitrocellulose membranes (Bio-Rad, 0.22 μM) for 1 hour at 100V. Membrane blots were blocked with phosphate-buffered saline containing 0.2% Tween-20 (vol/vol, PBS-T) and 5% nonfat milk (wt/vol, 5% milk) for 1 hour. Each membrane was incubated with rat anti-HA primary antibody (Sigma 11867423001; clone 3F10, monoclonal from Roche, 1:5,000 in 5% milk) overnight at 4°C . Blots were washed 3 \times for 5 minutes in PBS-T at room temperature. Licor anti-rat-680 secondary antibody (LICOR IRDye 680LT Goat Anti-Rat IgG (H + L), Highly Cross-Adsorbed; LIC-925-68029) was added for 1 hour at room temperature (1:15,000). Blots were washed 3 \times for 5 minutes in PBS-T at room temperature and

developed in the Odyssey Fc Imaging System (LI-COR Biosciences). All four mutants were used in preliminary comparative growth experiments with 2'-FL as described above; however, the clone that had the brightest band was named Akk-EH114 (MuT TnAmuc_2072::HHJ01_10880).

RESULTS

Evolutionary relationship of GHs involved in 2'-FL metabolism

Enzymes that target 2'-FL include fucosidases that cleave the α 1,2-linked fucose from the parent lactose, which can be further metabolized by a β -galactosidase. To identify mechanisms of 2'-FL degradation by human-associated *Akkermansia*, we first characterized the evolutionary relationship of predicted fucosidases belonging to the GH29 and GH95 families and β -galactosidases belonging to the GH2 family across species. A phylogenetic analysis revealed seven well-supported clades for GH29 and three for GH95 (Fig. 1). Generally, when each *Akkermansia* species was represented within a clade, strains from the same species clustered into sub-clades showing phylogenetic congruence for each species. An exception to this pattern is for the GH95 tree, where sequences of *A. bivaensis* were quite divergent within clade 3.

Representation of the strains across the clades was not uniform, where some *Akkermansia* species had greater numbers and diversity of fucosidases. Specifically, across the GH29 genes, *A. bivaensis* strains including strain CSUN-19 used in this study were present in 6 of the 7 clades including one clade (clade 4) found exclusively in this species (Table 1). By contrast, *A. muciniphila* strains, including the type strain MuC^T, were found in only 4 of 7 clades with none being exclusive to this species. Interestingly, however, clade 6 lacked sequences from either of these two representative species, but contained GH29 genes present in only phylogroup AmIb, a closely related sub-species of *A. muciniphila* previously defined by Becken and colleagues (38).

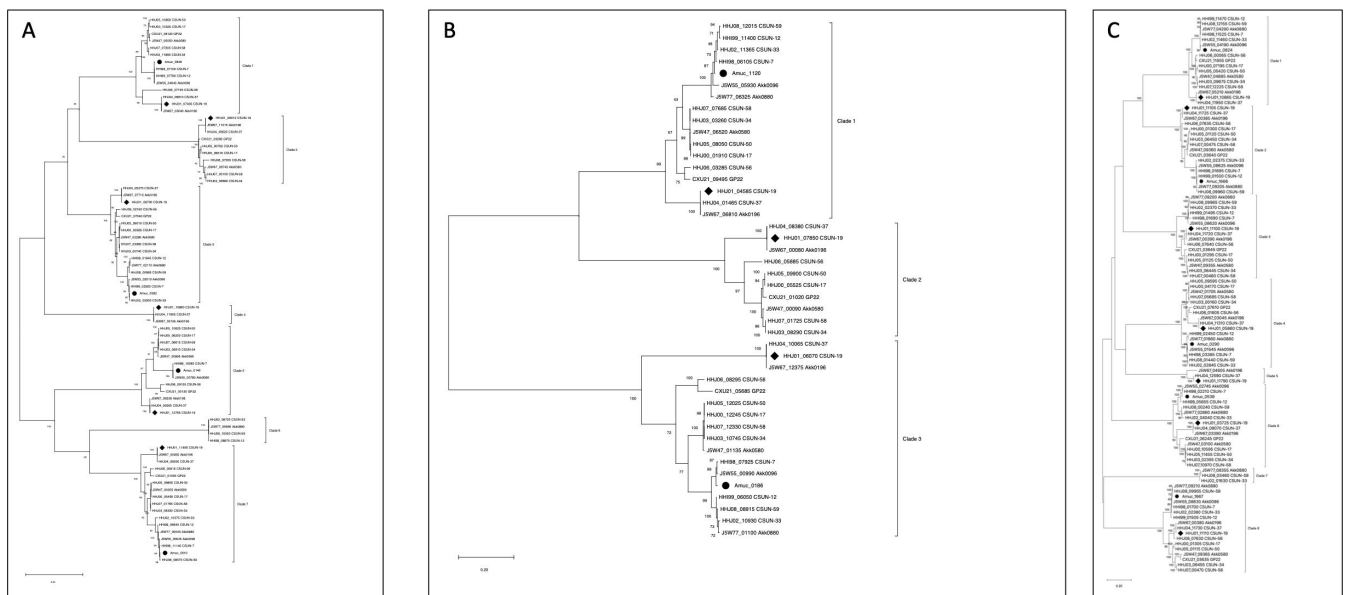


FIG 1 Maximum likelihood trees reveal seven clades of GH29 (A), three clades of GH95 (B), and eight clades of GH2 (C) genes across human-associated *Akkermansia* species. Sequences marked by circles represent genes from *A. muciniphila* MuC^T (AmI) and sequences marked by diamonds are genes from *A. bivaensis* CSUN-19 (AmIV), the representative strains used throughout this study. All trees were generated using a maximum likelihood heuristic method by executing Neighbor-Join and BioNJ (NJ/BioNJ) algorithms and applied to a matrix of pairwise distances with 100 bootstrap iterations. Trees are drawn to scale, with branch lengths measured in the number of substitutions per site. The trees in (A) involved 78 nucleotide sequences and a total of 3,258 positions in the final data set. For the tree in (B), 44 nucleotide sequences and 2,735 sites were analyzed, while in (C), 106 nucleotide sequences and 4,919 positions were included. Evolutionary analyses were conducted using MEGA11 (44–46).

TABLE 1 Presence of putative fucosidase (GH29 and GH95) and beta-galactosidase (GH2) genes in representative strains of the four species-level phylogroups reveals a greater suite of predicted fucosidases and beta-galactosidases in phylogroup IV (*A. biwaensis*) of human-associated *Akkermansia*^a

GH	Clade	Representative gene ID	Aml	AmlI	AmlII	AmlV
			(<i>A. muciniphila</i> Muc ^T)	(<i>A. massiliensis</i> CSUN17)	(<i>Akkermansia</i> sp. CSUN56)	(<i>A. biwaensis</i> CSUN19)
29	1	Amuc_0846	+	+	+	+
	2	CSUN19 HHJ01_08010		+	+	+
	3	Amuc_0392	+	+	+	+
	4	CSUN19 HHJ01_10880				+
	5	Amuc_0146	+	+	+	+
	6	CSUN33 HHJ02_08725				
	7	Amuc_0010	+	+	+	+
95	1	Amuc_1120	+	+	+	+
	2	CSUN19 HHJ01_07850		+	+	+
	3	Amuc_0186	+	+	+	+
2	1	Amuc_0824	+	+	+	+
	2	Amuc_1666	+	+	+	+
	3	CSUN19 HHJ01_11100		+	+	+
	4	Amuc_0290	+	+	+	+
	5	CSUN19 HHJ01_11790				+
	6	Amuc_0539	+	+		+
	7	CSUN33 HHJ02_01630				+
	8	Amuc_1667	+	+	+	+

^aClade designations are based on maximum likelihood trees (Fig. 1).

Similarly, in the GH95 tree, *A. massiliensis*, including strain CSUN-17, *Akkermansia* sp. CSUN-56 from phylogroup AmIII, and *A. biwaensis* including strain CSUN-19 had genes present in all three clades, whereas *A. muciniphila* including the type strain Muc^T, only had genes in two clades (Fig. 1; Table 1).

A similar phylogenetic analysis of GH2 genes in diverse *Akkermansia* revealed eight clades (Fig. 1). In line with previous findings, the representative species diverged, in which *A. muciniphila* Muc^T had fewer copies of GH2 (5/8 clades) (Table 1), and *A. biwaensis* CSUN-19 had the highest copy number of GH2s in the genome (7/8 clades). Each species also contained unique GH2 sequences; clade 5 was unique to *A. biwaensis* strains while clade 7 was unique to a subset of *A. muciniphila* strains in the Amlb subgroup (Fig. 1).

Growth of *A. muciniphila* Muc^T and *A. biwaensis* CSUN-19 on 2'-fucosyllactose and glucose

A. muciniphila and *A. biwaensis*, the two species with the most divergent number of predicted fucosidases, were used to determine the relative growth and generation of sugar metabolites in a minimal media with 2'-FL. Interestingly, although both strains grew using 2'-FL and GlcNAc, the final OD_{600nm} was different across species. By 36 hours, the OD_{600nm} of *A. biwaensis* CSUN-19 was nearly double that of *A. muciniphila* Muc^T (Fig. 2). Although we are unable to calculate a formal growth rate because of sparse sampling, *A. biwaensis* CSUN-19 reached a final OD ≥ 1.5 by 36 hours, whereas by 120 hours, *A. muciniphila* Muc^T had yet to reach this level of growth. This contrasts with the growth on Glc and GlcNAc, where both species reached similar densities across all time points (Fig. S2).

We tested whether these species were degrading and consuming the available sugars through similar pathways by measuring the concentrations of the various oligosaccharides (e.g., 2'-FL, lactose) and monosaccharides (e.g., Glc, galactose, GlcNAc). Both strains degraded 2'-FL into fucose and lactose and consumed nearly all GlcNAc by the end of the experiment. Although lactose and fucose were found in the culture medium during growth on 2'-FL, fucose was quickly consumed, whereas lactose accumulated in cultures from both organisms (Fig. 2). In addition, small but appreciable amounts of glucose

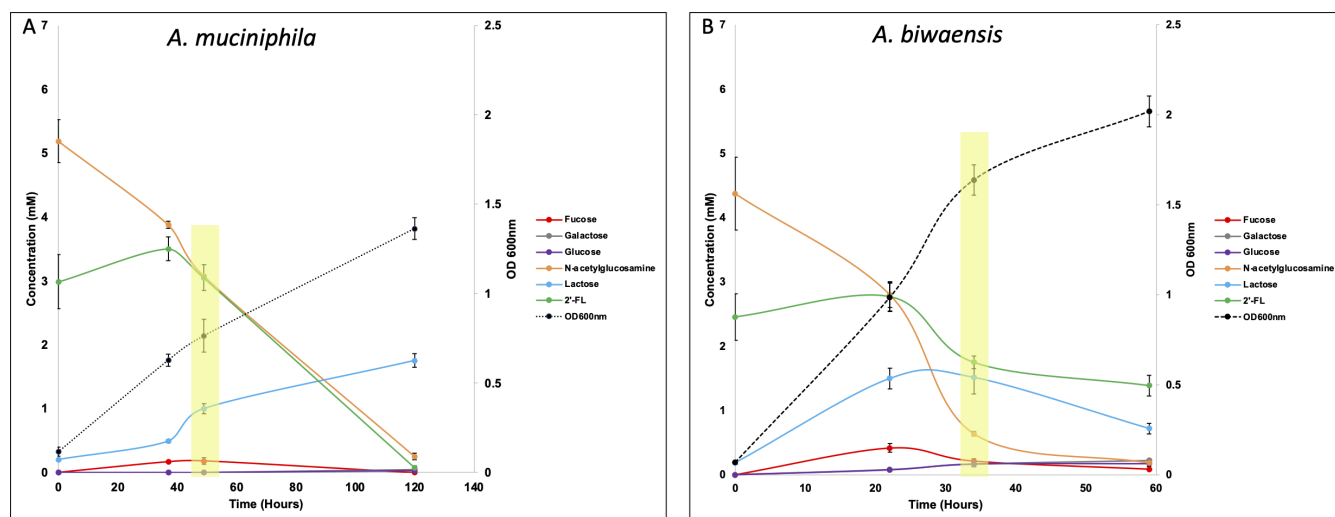


FIG 2 *A. muciniphila* Muc^T and *A. biwaensis* CSUN-19 use 2'-FL and GlcNAc for growth. Fucose, lactose, glucose, and galactose, breakdown products of 2'-FL degradation, are detectable in culture media during different stages of growth. Note the differences in time along the y-axis. Highlighting Asterisks denotes time points where cells were collected for RNAseq. Error bars represent the standard deviation of triplicate cultures.

and galactose accumulated in the culture medium of *A. biwaensis* CSUN-19 but not *A. muciniphila* Muc^T. As anticipated, when grown on glucose and GlcNAc, both strains consumed these sugars within 34 hours of growth (Fig. S2) (25).

Gene regulation of *A. muciniphila* Muc^T and *A. biwaensis* on 2'-fucosyllactose and glucose

We performed an RNAseq analysis of both *A. muciniphila* Muc^T and *A. biwaensis* CSUN-19 during mid-log growth on GlcNAc and either Glc or 2'-FL. Because the strains grew at different rates in the different media backgrounds, RNA was extracted from cells harvested during mid-log growth (shading, Fig. 2; Fig. S2). Importantly, 2'-FL was present in the culture media at the time of sampling, indicating that consumption of this HMO was ongoing. The quality and quantity of all RNA extracts varied but sequencing yields were consistent across samples averaging approximately 15 million reads per sample (Table S4). On average, across all samples, 38% of the total reads were aligned to coding sequences (CDs) of each genome. Compared to growth on glucose, 146 of 2,115 (~6.9%) genes were differentially expressed by *A. muciniphila* Muc^T when grown on 2'-FL, of which 51 were downregulated and 95 were upregulated (Fig. S3). Analysis of *A. biwaensis* CSUN-19 identified 507 out of 2,557 (~21%) differentially expressed genes when grown on 2'-FL versus glucose, of which 302 were downregulated and 225 were upregulated.

Initial analysis of the top 20 most differentially expressed genes for each strain revealed limited overlap (highlighted rows, Tables S5 and S6). Within the top 20 most differentially expressed genes of *A. muciniphila* Muc^T, multiple GHs were identified including a GH2 (putative beta-galactosidase), GH16 (active on β -1,4 or β -1,3 glycosidic bonds), and a GH88 (putative glucuronidase), as well as multiple hypothetical proteins, a putative surface layer protein, and two NADPH-dependent oxidoreductases. By contrast, for *A. biwaensis* CSUN-19, none of the top 20 most differentially expressed genes encoded for GHs, instead constituting mostly genes related to iron transport and annotated as hypothetical proteins.

An analysis of the predicted fucosidases, GH29 and GH95 families, revealed that in *A. muciniphila* Muc^T only Amuc_0846 was significantly upregulated when grown on 2'-FL (\log_2 fold change $>|2|$, $P_{\text{adj}} < 0.05$), and none of the GH95 genes were significantly regulated (Table 2). For *A. biwaensis* CSUN-19, three GH29 genes were significantly upregulated (\log_2 fold change $>|2|$, $P_{\text{adj}} < 0.05$), and one GH29 and one GH95 gene were

TABLE 2 A subset of glycoside hydrolases are regulated in the presence of 2'-FL^a

<i>A. muciniphila</i> Muc ^T						<i>A. biwaensis</i> CSUN-19					
Annotation	Clade	geneID	log2FC	AveExpr	Adj.P.val	Annotation	Clade	geneID	log2FC	AveExpr	Adj.P.val
GH29	1	Amuc_0846	4.52	3.62	1.28 × 10 ⁻⁵	GH29	1	HHJ01_07405	2.02	5.20	1.33 × 10 ⁻⁷
GH29	3	Amuc_0392	1.20	9.30	1.17 × 10 ⁻³	GH29	2	HHJ01_08010	1.64	6.48	2.42 × 10 ⁻⁹
GH29	5	Amuc_0146	0.18	5.21	4.97 × 10 ⁻¹	GH29	3	HHJ01_06700	-0.75	8.68	1.81 × 10 ⁻⁶
GH29	7	Amuc_0010	-0.46	8.21	6.91 × 10 ⁻²	GH29	4	HHJ01_10880	2.59	5.25	7.08 × 10 ⁻¹⁰
GH95	1	Amuc_1120	1.18	9.82	6.00 × 10 ⁻³	GH29	5	HHJ01_12765	2.12	5.66	1.19 × 10 ⁻⁷
GH95	3	Amuc_0186	1.77	7.63	3.91 × 10 ⁻⁵	GH29	7	HHJ01_11495	-2.55	6.55	4.25 × 10 ⁻¹¹
GH2	1	Amuc_0824	0.01	11.14	9.71 × 10 ⁻¹	GH95	1	HHJ01_04585	-1.26	8.76	5.24 × 10 ⁻⁸
GH2	2	Amuc_1666	2.55	3.98	6.13 × 10 ⁻⁵	GH95	2	HHJ01_07850	-2.58	5.04	6.08 × 10 ⁻¹⁰
GH2	4	Amuc_0290	0.85	10.55	7.66 × 10 ⁻³	GH95	3	HHJ01_06070	-0.44	7.08	1.74 × 10 ⁻³
GH2	6	Amuc_0539	3.77	8.38	1.34 × 10 ⁻⁶	GH2	1	HHJ01_10865	-0.45	9.88	2.23 × 10 ⁻⁴
GH2	8	Amuc_1667	1.98	5.30	1.34 × 10 ⁻⁴	GH2	2	HHJ01_11105	-0.65	8.07	2.19 × 10 ⁻⁵
						GH2	3	HHJ01_11110	1.60	5.89	4.54 × 10 ⁻⁷
						GH2	4	HHJ01_05860	0.23	11.61	6.09 × 10 ⁻²
						GH2	5	HHJ01_11790	-0.59	8.91	1.67 × 10 ⁻⁵
						GH2	6	HHJ01_03725	0.63	9.23	1.82 × 10 ⁻⁵
						GH2	8	HHJ01_11100	-0.65	7.57	2.50 × 10 ⁻⁵

^aRNAseq analysis of the expression of genes encoding glycoside hydrolases potentially involved in 2'-FL metabolism including fucosidases, such as GH29 and GH95, and β-galactosidases, such as GH2. Fold change (log2FC) in gene expression compared to mid-log growth on glucose for both *A. muciniphila* Muc^T and *A. biwaensis* CSUN-19. Average Expression for these genes is based on growth across both conditions. Shaded rows indicate genes that are significantly regulated by 2'-FL.

significantly downregulated. The β-galactosidase family GH2 is also likely to be involved in lactose metabolism once fucose is liberated from 2'-FL. Our analysis indicated that two genes, Amuc_1666 and Amuc_0539 were significantly upregulated in *A. muciniphila* Muc^T during growth on 2'-FL, whereas GH2 genes in *A. biwaensis* CSUN-19 were not significantly upregulated.

Genomic loci of GH2 and GH29/GH95 genes across human-associated *Akkermansia*

The differences in 2'-FL degradation across species may also be due to genetic variation between the strains; therefore, we compared the genomic locus of *A. biwaensis* CSUN-19 containing the most differentially upregulated GH29 (HHJ01_10880) across all four known human-associated *Akkermansia* species (Fig. 3). Surprisingly, *A. biwaensis* CSUN-19 was the only species containing this GH29 (HHJ01_10880), agreeing with our phylogenetic analysis. However, all four species have a GH2 β-galactosidase (*A. muciniphila* Muc^T = Amuc_0824; *A. biwaensis* CSUN-19 = HHJ01_10865) within the same genomic locus that may be involved in the cleavage of the lactose after removal of the terminal fucose. In addition to the GH2, *A. biwaensis* CSUN-19, *A. massiliensis* CSUN-17, and *Akkermansia* sp. CSUN-56 have genes in this locus encoding a hypothetical protein that is likely a putative sialidase upon further BLASTp search (blue, Fig. 3). These same three species

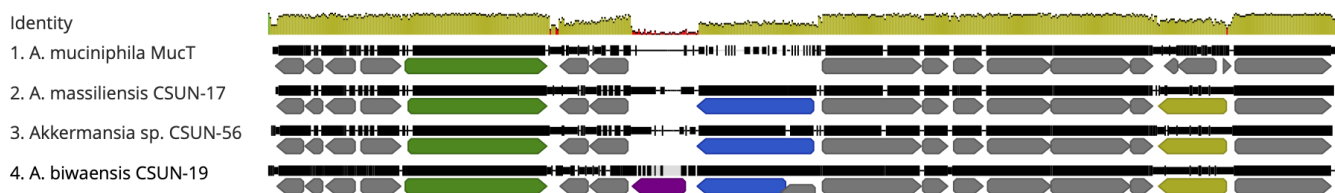


FIG 3 Genomic region containing the 2'-FL-regulated GH29 is absent in *A. muciniphila*. Structure and similarity of the locus containing predicted GH2 and GH29 genes between *A. muciniphila* Muc^T, *A. massiliensis* CSUN-17, *Akkermansia* sp. CSUN-56, and *A. biwaensis* CSUN-19. Alignment made with Geneious using default parameters. All annotated open reading frames are depicted in gray with the following predicted CAZymes: GH2 (green), GH29 (purple), GH33 (blue), GH27 (yellow). The region represented is bound by the following genes: Amuc-0820 and Amuc-0836 (Muc^T), HHJ00_07175 and HHJ00_07250 (CSUN-17), HHJ06_00085 and HHJ06_00010 (CSUN-56), HHJ01_10845, and HHJ01_10930 (CSUN-19).

that retain the putative sialidase also encode a putative α -galactosidase approximately 7 kb upstream (yellow, Fig. 3). Interestingly, *A. muciniphila* Muc^T is missing all three of these putative glycoside hydrolases.

Characterization of 2'-FL degrading proteins from *A. biwaensis* CSUN-19

Next, we aimed to characterize the putative β -galactosidase (HHJ01_10865) and putative α -fucosidase (HHJ01_10880) from *A. biwaensis* CSUN-19 that are likely involved in 2'-FL degradation. Toward this, we cloned and purified the putative β -galactosidase, HHJ01_10865 without its signal peptide and determined its enzymatic activity toward ortho-Nitrophenyl- β -galactoside (ONPG). β -galactosidase activity was observed for HHJ01_10865 (Fig. S4A) in a dose-dependent manner with an optimal pH range of 6.0 to 8.0 and MgCl₂ dependence (Fig. S4B).

Similar cloning and protein purification was completed with the putative α -fucosidase (HHJ01_10880) but all attempts at characterizing activity on para-nitrophenyl- α -L-fucoside (pNPFuc) and 2'-FL were unsuccessful (data not shown). Phylogenetic comparisons

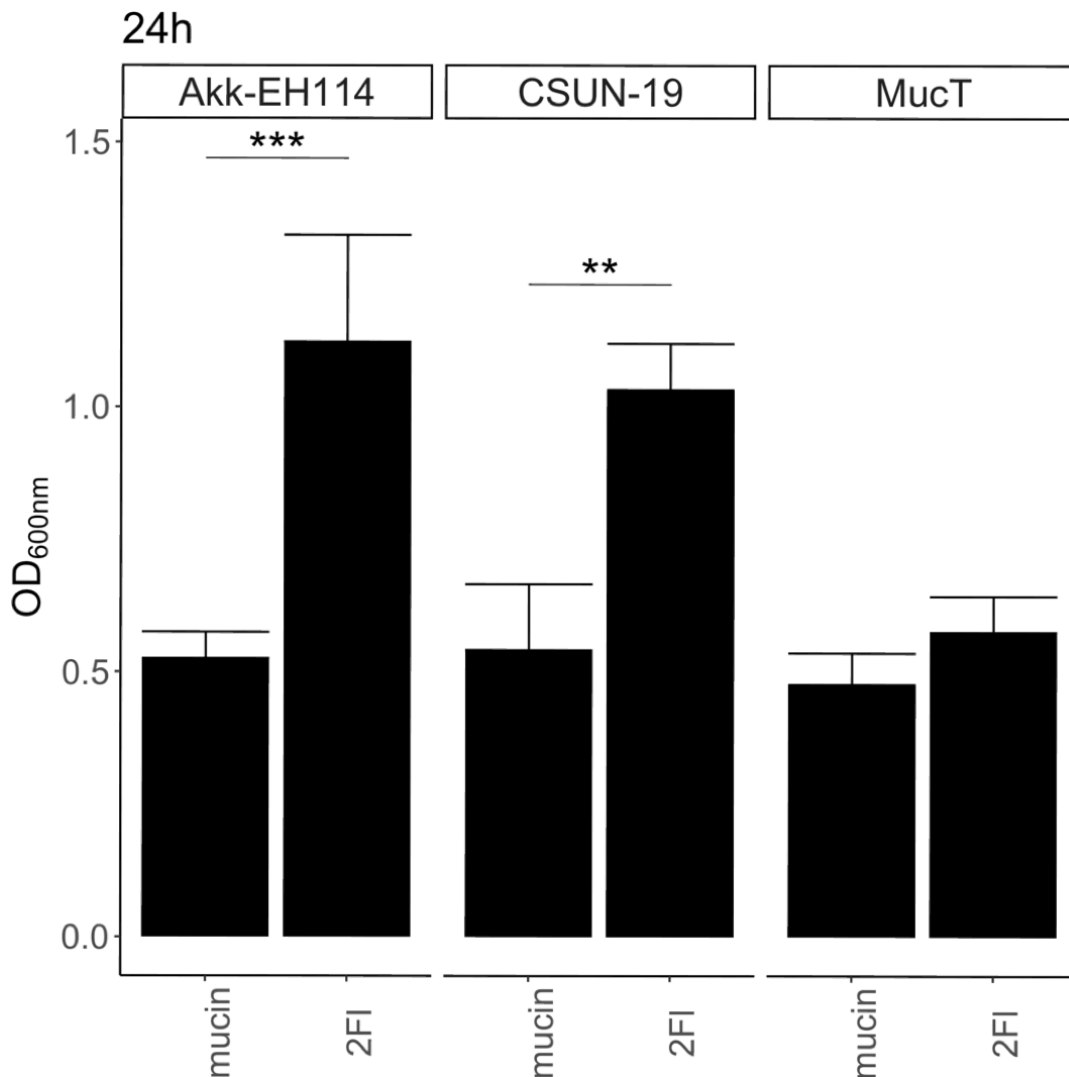


FIG 4 Expression of the *A. biwaensis* GH29 gene in *A. muciniphila* enhances growth on 2'-FL. *A. muciniphila* Muc^T, *A. biwaensis* CSUN-19, and *A. muciniphila* Akk-EH114 (Muc^T expressing HHJ01_10880). Cultures were inoculated into BTM containing a final concentration of 0.4% mucin and 10 mM 2'-FL. OD_{600nm} was measured at 0 and 24 hours and normalized to the 0-hour time point. Error bars represent the standard deviation of three biological replicates. Statistically significant differences are calculated by Tukey's multiple comparisons test with $P < 0.05$. Symbol style: 0.1 (***) and 0.001 (**).

of HHJ01_10880 with related GH29 enzymes from other intestinal bacteria suggest that this enzyme is a GH29B enzyme (Fig. S5) and may require an additional binding of a second sugar. To determine the role of HHJ01_10880 in 2'-FL catabolism, we used a complementary approach of expressing the *A. biwaensis* putative fucosidase in *A. muciniphila* Muc^T. A transposon-based HHJ01_10880 expression construct was delivered by conjugation into *A. muciniphila* Muc^T. The insertion sites of the Tn insertions from four clones were confirmed, and all four clones were used to assess growth in BTTM + 0.4% mucin supplemented with or without 2'-FL across a 48-hour period (Fig. S6). One clone (Akk- EH114) had comparable growth to *A. muciniphila* Muc^T in background conditions but grew significantly better on 2'-FL (Fig. 4), similar to the growth of *A. biwaensis* CSUN-19 on 2'-FL. Together, these results suggest this enzyme is involved in 2'-FL catabolism.

DISCUSSION

One important function of HMOs is to facilitate the expansion of beneficial bacteria in the gut microbiota early in life. Recently, different species of human-associated *Akkermansia* have been shown to grow using HMOs (26, 27), expanding their ecological niche and potential importance in the development of the human gut. The mechanisms by which *Akkermansia* uses HMOs, specifically the highly abundant 2'-FL, may affect how they interact in and shape both the composition of the infant gut microbiota and the development of the infant. Here, we used comparative genomics, phenotypic and transcriptomic profiling, and enzyme activity assays to explore the mechanisms of 2'-FL catabolism in human-associated *Akkermansia* species. We found that strains of *A. biwaensis* possess a higher diversity of both putative fucosidase (GH29 and GH95) and β -galactosidase (GH2) encoding genes than other *Akkermansia* species. Despite this genomic difference, both *A. muciniphila* Muc^T and *A. biwaensis* CSUN-19 grew in 2'-FL in media lacking mucin. Furthermore, both strains significantly induced the expression of homologs of a gene encoding a GH29 fucosidase (clade 1), for which the purified protein from *A. muciniphila* has previously been shown to have weak activity against para-nitrophenyl- α -L-fucoside, an analog of 2'-FL (32). Interestingly, a gene unique to *A. biwaensis* strains encoding a different GH29 was also significantly upregulated on 2'-FL. Importantly, expression of this GH29 in *A. muciniphila* was sufficient to enhance its growth to levels similar to *A. biwaensis* in 2'-FL. An additional gene encoding a putative GH2 gene in the same genomic region as the differentially expressed GH29 was confirmed to be a β -galactosidase which is needed to fully deconstruct the 2'-FL trisaccharide. Surprisingly, *A. biwaensis* had a significantly downregulated GH95 fucosidase despite its importance in 2'-FL catabolism. Overall, these findings highlight the different strategies used by *Akkermansia* species to deconstruct fucose-containing HMOs and point to functional differences that may influence the colonization success and health impacts of *Akkermansia* at different host life stages.

GH29 and GH95 family proteins are involved in 2'-FL catabolism

Analysis of putative fucosidase and β -galactosidase genes across *Akkermansia* species revealed differences in the number and diversity of GH29, GH95, and GH2 genes that were phylogroup specific. Recently, six fucosidases (four GH29 and two GH95 enzymes) from *A. muciniphila* Muc^T have been characterized, demonstrating each enzyme has specific activity on different fucosylated substrates that are diet- or host-derived (32). These corroborate previous work demonstrating that members of the GH95 family preferentially hydrolyze 1,2- α -L-fucosylated linkages (70). By contrast, the other dominant fucosidase family, GH29, is divided into two subfamilies, GH29A and GH29B (49, 50), in which Group A has little substrate specificity and GH29 Group B preferentially hydrolyzes α -1,3/1,4-L-fucosidase linkages (71, 72). Typically, GH29A enzymes show broader linkage specificity than the GH29B enzymes that show preference for α -1,3/4 fucosylated linkages. However, these linkage preferences are not absolute and many GH29B enzymes have broad substrate activities. Furthermore, we find that *A.*

massiliensis CSUN-17, *Akkermansia* sp. CSUN-56, and *A. biwaensis* CSUN-19 contain more copies of both GH29 and GH95 genes than *A. muciniphila* Muc^T, suggesting the capacity to metabolize a broader set of fucosylated substrates or under a broader range of conditions, such as pH or temperature. Several studies have demonstrated the optimal performance of fucosidases, sialidases, neuraminidases, β -galactosidases, and β -acetylhexosaminidases from multiple organisms, including *Akkermansia*, at specific pH values (26, 72, 73) and fucosidases with different activity depending on the temperature (74). Given that the local pH will vary along the length of the infant intestine, it is therefore necessary to understand the conditions under which these enzymes are expressed to model colonization dynamics (75).

Fucosidase expression patterns observed in *A. muciniphila* Muc^T and *A. biwaensis* CSUN-19 under 2'-FL growth conditions suggest that GH29 are the primary enzymes responsible for the cleavage of the terminal fucose residue. In our phylogenetic analysis, genes from clade 1 were significantly upregulated in both species. Interestingly, this protein in *A. muciniphila* Muc^T, Amuc_0846, has weak activity on 2'-FL but strong mucin binding activity (32). Also in agreement, both strains downregulated (significantly only for *A. biwaensis* CSUN-19) another GH29 belonging to clade 7. Previous reports of this purified protein from *A. muciniphila* Muc^T, Amuc_0010, demonstrated very weak activity of this purified enzyme against 2'-FL (26, 32). Our results further support these findings suggesting that this fucosidase may not be the primary enzyme for 2'-FL catabolism.

While there were similarities in fucosidase expression patterns across species, there were also notable differences. Most notable was the significant upregulation of HHJ01_10880 in *A. biwaensis* CSUN-19, a predicted GH29B fucosidase absent in other *Akkermansia* species. The purified HHJ01_10880 did not display fucosidase activity using both a substrate analog and the synthetic 2'-FL used in growth experiments. However, other purified GH29B enzymes from intestinal bacteria are not active on chromogenic substrates and often have a second binding pocket that must be occupied by a second sugar for efficient fucosidase activity (70). For example, the GH29B enzymes that share sequence similarity to HHJ01_10880 (Fig. S5) from *Bacteroides thetaiotaomicron* (BT_2192) and *Ruminococcus gnavus* (E1_10125) bind β -D-galactose and sialic acid, respectively, during catabolism of fucosylated substrates (51, 54). Thus, this inability to detect the activity of purified HHJ01_10880 was not unexpected, and further work is needed to characterize fucosidase activity with HMO sugar combinations.

β -galactosidases involved in 2'-FL catabolism

Expression levels of the GH2 (HHJ01_10865) located in the same genomic region of *A. biwaensis* CSUN-19 were high but not induced by 2'-FL. The activity we observe for recombinant GH2 HHJ01_10865 is similar to other β -galactosidases from HMO-degrading microorganisms (33, 76). This family of enzymes includes proteins with a wide range of activities including β -galactosidase (EC 3.2.1.23), β -mannosidase (EC 3.2.1.25), β -glucuronidase (EC 3.2.1.31), and *exo*- β -glucosaminidase (EC 3.2.1.-) (77). *Akkermansia* harbors other β -galactosidases, such as the GH35 family, that are active on β (1, 3)- and β (1, 6)- galactoside linkages (78, 79). While the GH35 family is unlikely to target the lactose backbone, HMOs such as Lacto-N-tetraose and Lacto-N-neotetraose, that have a β (1, 3) or (1, 6) galactoside linkage to N acetyl glucosamine, may be targeted. These linkages are also present in mucin (80), which may implicate β -galactosidases in the metabolism of both glycan types. Recently, comparative growth of Tn knockouts in 38 GHs indicated that about 80% of these were not essential for the growth on mucin (67). Together with the number, diversity, and shared functions across multiple enzymes, it suggests GH redundancy in *Akkermansia*. Future work using *A. muciniphila* Muc^T as a genetic system to express full-length glycoside hydrolases may be used to accurately determine the functional range of these enzymes.

Genomic linkage of GH genes involved in HMO metabolism

For *Akkermansia* species CSUN-19, the most differentially expressed GH29 when grown on 2'-FL was the predicted fucosidase HHJ01_10880. Interestingly, in the same genomic region as HHJ01_10880, there is also a β -galactosidase 3 genes downstream (Fig. 3), albeit on the opposite DNA strand. While this β -galactosidase was not differentially expressed under 2'-FL growth conditions, it was among the most highly expressed genes for both organisms (Table 2). In other Gram-negative HMO-degrading bacteria including *Bacteroides*, HMO-active GH genes are genomically co-localized and co-regulated in polysaccharide utilization loci (PUL) to efficiently respond to available carbohydrates (23). PULs also contain substrate-binding proteins and transport proteins for the target polysaccharides. *Akkermansia* do not have this typical PUL organization despite several GHs mapping to this region. However, given the regional proximity and high abundance of both transcripts when grown on 2'-FL, we propose a model in which the HHJ01_10880 cleaves the fucose by breaking the α 1–2 bond, leaving the residual lactose (β 1–4) to be cleaved by the adjacent β -galactosidase (HHJ01_10865). Based on the presence of signal peptide sequences, we predict that both the GH29 and the GH2 operate in the periplasmic or extracellular space (26, 67). With this proposed model, after extracellular cleavage of fucose, the lactose would have to be further processed by the β -galactosidase before cellular uptake. Supporting this model, the genome of *A. biwaensis* CSUN-19 lacks an ortholog of the LacY permease, suggesting lactose is not likely imported into the cytoplasm. While this is the first report of introducing and expressing genes in *A. muciniphila* based on the recently developed genetic modification system (67), expansion of this method to include targeted gene knockouts in *A. biwaensis* is eagerly anticipated to confirm this model. Alternatively, understanding the movement of sugar in these systems would be greatly improved by labeled substrates that can be tracked in real time through the cell.

Conclusions

The presence of *Akkermansia* in infants may be correlated with its ability to utilize HMOs. In this study, *Akkermansia* isolates from two divergent species, *A. muciniphila* and *A. biwaensis*, were shown to have different growth dynamics on 2'-FL, an abundant HMO in breastmilk. Phylogenetic analysis of putative fucosidases (GH29 and GH95) and β -galactosidases (GH2) involved with the deconstruction of 2'-FL coupled with transcriptional profiling pointed to two genes in a genomic locus that may be responsible for enhanced growth of *A. biwaensis*. We provide evidence that a GH29 present in *A. biwaensis* but absent in *A. muciniphila* is most likely responsible for this phenotype and that both this GH29 and an associated β -galactosidase perform their activities extracellularly (26). In addition to serving as a substrate for *Akkermansia* GH2 enzymes, in a complex ecosystem, the released lactose could also serve as a substrate for other members of the infant microbiota. A healthy adult gut microbiome begins in early life where it is shaped by human milk sugars through glycan-degrading microbes. The difference in *Akkermansia* species to break down HMOs suggests a species-specific role in the development of a healthy microbiome. This is significant because it points to the strain-specific mechanisms by which *Akkermansia* may colonize and shape the infant gut, ultimately leading to the rational selection of probiotic bacteria and prebiotic therapies.

ACKNOWLEDGMENTS

The authors would like to thank Egle Pakalnyte and Louise Vigsnaes of Glycom for their generous donation of HMOs and their continued support of our work. Thank you to Mike Summers and Melissa Takahashi for providing strains of *E. coli*. Lastly, we would like to thank all current and past members of the Flores lab for the many discussions regarding this project.

This work was supported by the National Institutes of Health through the National Institute of General Medical Sciences (NIGMS) [grant number SC1GM136546] awarded

to G.E.F. and the National Institute of Allergy and Infectious Diseases (NIAID) [grant number AI142376] awarded to R.H.V. E.R.H. is a Robert Black Fellow of the Damon Runyon Cancer Research Foundation, DRG-2455-22. The content is solely the responsibility of the authors and does not necessarily represent the official views of the National Institutes of Health.

Conceptualization, G.E.F. and L.P.; methodology, G.E.F., L.P., A.D.F., E.H., and R.H.V.; formal analysis and investigation, G.E.F., A.D.F., L.P., E.L., and B.C.; visualization, G.E.F., A.D.F., and L.P.; supervision, G.E.F. and R.H.V. All authors provided critical feedback and helped shape the research, analysis, and manuscript. All authors have read and agreed to the published version of the manuscript.

AUTHOR AFFILIATIONS

¹Department of Biology, California State University, Northridge, California, USA

²GlycoAnalytics Core, UC San Diego, Health Sciences, La Jolla, California, USA

³Department of Integrative Immunobiology, Duke University School of Medicine, Durham, North Carolina, USA

AUTHOR ORCIDs

Ashwana D. Fricker  <http://orcid.org/0000-0002-3806-7695>

Gilberto E. Flores  <http://orcid.org/0000-0002-3338-611X>

FUNDING

Funder	Grant(s)	Author(s)
HHS NIH National Institute of General Medical Sciences (NIGMS)	SC1GM136546	Loren Padilla Ashwana D. Fricker Estefani Luna Gilberto E. Flores
HHS NIH National Institute of Allergy and Infectious Diseases (NIAID)	AI142376	Elizabeth R. Hughes Maria E. Panzetta Raphael H. Valdivia

AUTHOR CONTRIBUTIONS

Loren Padilla, Formal analysis, Investigation, Methodology, Writing – original draft, Writing – review and editing | Ashwana D. Fricker, Formal analysis, Investigation, Methodology, Validation, Visualization, Writing – original draft, Writing – review and editing | Estefani Luna, Investigation, Methodology, Writing – original draft | Biswa Choudhury, Investigation, Methodology | Elizabeth R. Hughes, Investigation, Methodology, Visualization | Maria E. Panzetta, Investigation, Methodology | Raphael H. Valdivia, Funding acquisition, Project administration, Resources, Supervision, Writing – review and editing | Gilberto E. Flores, Conceptualization, Data curation, Formal analysis, Funding acquisition, Methodology, Project administration, Supervision, Visualization, Writing – original draft, Writing – review and editing

DATA AVAILABILITY

Data that support the findings of this study are openly available in the NCBI BioProject database at SRA, accession number [PRJNA1023561](#).

ETHICS APPROVAL

This research has complied with all institutional and federal policies regarding the use of human subjects.

ADDITIONAL FILES

The following material is available [online](#).

Supplemental Material

File S1 (JB00334-23-s0001.html). R markdown file of basic code and outputs produced during analysis of *A. muciniphila* MucT.

File S2 (JB00334-23-s0002.html). R markdown file of basic code and outputs produced during analysis of *A. biwaensis* CSUN-19.

Supplemental figures (JB00334-23-s0003.pdf). Figures S1 to S6.

Tables S5 and S6 (JB00334-23-s0004.xlsx). Differentially expressed genes of *A. muciniphila* MucT and *A. biwaensis* CSUN-19.

Tables S1 to S4 (JB00334-23-s0005.pdf). Accession information for phylogenetic analyses and read information from RNAseq.

Supplemental legends (JB00334-23-s0006.pdf). Legends for all supplemental material.

REFERENCES

- Breastfeeding. UNICEF data. Available from: <https://data.unicef.org/topic/nutrition/breastfeeding>. Retrieved 8 Aug 2023.
- Ballard O, Morrow AL. 2013. Human milk composition: nutrients and bioactive factors. *Pediatr Clin North Am* 60:49–74. <https://doi.org/10.1016/j.pcl.2012.10.002>
- Garwolińska D, Namieśnik J, Kot-Wasik A, Hewelt-Belka W. 2018. Chemistry of human breast milk—a comprehensive review of the composition and role of milk metabolites in child development. *J Agric Food Chem* 66:11881–11896. <https://doi.org/10.1021/acs.jafc.8b04031>
- Kim SY, Yi DY. 2020. Components of human breast milk: from macronutrient to microbiome and microRNA. *Clin Exp Pediatr* 63:301–309. <https://doi.org/10.3345/cep.2020.00059>
- Hegar B, Wibowo Y, Basrowi RW, Ranuh RG, Sudarmo SM, Munasir Z, Atthiyah AF, Widodo AD, Supriatmo, Kadim M, Suryawan A, Diana NR, Manoppo C, Vandenplas Y. 2019. The role of two human milk oligosaccharides, 2'-fucosyllactose and lacto-N-neotetraose, in infant nutrition. *Pediatr Gastroenterol Hepatol Nutr* 22:330–340. <https://doi.org/10.5223/pghn.2019.22.4.330>
- Brand-Miller JC, McVeagh P, McNeil Y, Messer M. 1998. Digestion of human milk oligosaccharides by healthy infants evaluated by the lactulose hydrogen breath test. *J Pediatr* 133:95–98. [https://doi.org/10.1016/s0022-3476\(98\)70185-4](https://doi.org/10.1016/s0022-3476(98)70185-4)
- Engfer MB, Stahl B, Finke B, Sawatzki G, Daniel H. 2000. Human milk oligosaccharides are resistant to enzymatic hydrolysis in the upper gastrointestinal tract. *Am J Clin Nutr* 71:1589–1596. <https://doi.org/10.1093/ajcn/71.6.1589>
- Ward RE, Niñonuevo M, Mills DA, Lebrilla CB, German JB. 2007. *In vitro* fermentability of human milk oligosaccharides by several strains of bifidobacteria. *Mol Nutr Food Res* 51:1398–1405. <https://doi.org/10.1002/mnfr.200700150>
- Kunz C, Rudloff S. 1993. Biological functions of oligosaccharides in human milk. *Acta Paediatr* 82:903–912. <https://doi.org/10.1111/j.1651-2227.1993.tb12597.x>
- Wu S, Tao N, German JB, Grimm R, Lebrilla CB. 2010. Development of an annotated library of neutral human milk oligosaccharides. *J Proteome Res* 9:4138–4151. <https://doi.org/10.1021/pr100362f>
- Wu S, Grimm R, German JB, Lebrilla CB. 2011. Annotation and structural analysis of sialylated human milk oligosaccharides. *J Proteome Res* 10:856–868. <https://doi.org/10.1021/pr101006u>
- Totten SM, Zivkovic AM, Wu S, Ngyuen U, Freeman SL, Ruhaak LR, Darboe MK, German JB, Prentice AM, Lebrilla CB. 2012. Comprehensive profiles of human milk oligosaccharides yield highly sensitive and specific markers for determining secretor status in lactating mothers. *J Proteome Res* 11:6124–6133. <https://doi.org/10.1021/pr300769g>
- Vinjamuri A, Davis JCC, Totten SM, Wu LD, Klein LD, Martin M, Quinn EA, Scelza B, Breakey A, Gurven M, Jasienska G, Kaplan H, Valeggia C, Hinde K, Smilowitz JT, Bernstein RM, Zivkovic AM, Barratt MJ, Gordon JI, Underwood MA, Mills DA, German JB, Lebrilla CB. 2022. Human milk oligosaccharide compositions illustrate global variations in early nutrition. *J Nutr* 152:1239–1253. <https://doi.org/10.1093/jn/nxac027>
- Triantis V, Bode L, van Neerven RJJ. 2018. Immunological effects of human milk oligosaccharides. *Front Pediatr* 6:190. <https://doi.org/10.3389/fped.2018.00190>
- Morrison DJ, Preston T. 2016. Formation of short chain fatty acids by the gut microbiota and their impact on human metabolism. *Gut Microbes* 7:189–200. <https://doi.org/10.1080/19490976.2015.1134082>
- Sela DA, Chapman J, Adeuya A, Kim JH, Chen F, Whitehead TR, Lapidus A, Rokhsar DS, Lebrilla CB, German JB, Price NP, Richardson PM, Mills DA. 2008. The genome sequence of *Bifidobacterium longum* subsp. *infantis* reveals adaptations for milk utilization within the infant microbiome. *Proc Natl Acad Sci U S A* 105:18964–18969. <https://doi.org/10.1073/pnas.0809584105>
- Milani C, Duranti S, Bottacini F, Casey E, Turroni F, Mahony J, Belzer C, Delgado Palacio S, Arboleya Montes S, Mancabelli L, Lugli GA, Rodriguez JM, Bode L, de Vos W, Gueimonde M, Margolles A, van Sinderen D, Ventura M. 2017. The first microbial colonizers of the human gut: composition, activities, and health implications of the infant gut microbiota. *Microbiol Mol Biol Rev* 81:e00036-17. <https://doi.org/10.1128/MMBR.00036-17>
- Schwab C. 2022. The development of human gut microbiota fermentation capacity during the first year of life. *Microb Biotechnol* 15:2865–2874. <https://doi.org/10.1111/1751-7915.14165>
- Kirmiz N, Robinson RC, Shah IM, Barile D, Mills DA. 2018. Milk glycans and their interaction with the infant-gut microbiota. *Annu Rev Food Sci Technol* 9:429–450. <https://doi.org/10.1146/annurev-food-030216-030207>
- Thomson P, Medina DA, Garrido D. 2018. Human milk oligosaccharides and infant gut bifidobacteria: molecular strategies for their utilization. *Food Microbiol* 75:37–46. <https://doi.org/10.1016/j.fm.2017.09.001>
- Ruiz-Moyano S, Totten SM, Garrido DA, Smilowitz JT, German JB, Lebrilla CB, Mills DA. 2013. Variation in consumption of human milk oligosaccharides by infant gut-associated strains of *Bifidobacterium breve*. *Appl Environ Microbiol* 79:6040–6049. <https://doi.org/10.1128/AEM.01843-13>
- Garrido D, Ruiz-Moyano S, Kirmiz N, Davis JC, Totten SM, Lemay DG, Ugalde JA, German JB, Lebrilla CB, Mills DA. 2016. A novel gene cluster allows preferential utilization of fucosylated milk oligosaccharides in *Bifidobacterium longum* subsp. *longum* SC596. *Sci Rep* 6:35045. <https://doi.org/10.1038/srep35045>
- Marcobal A, Barboza M, Sonnenburg ED, Pudlo N, Martens EC, Desai P, Lebrilla CB, Weimer BC, Mills DA, German JB, Sonnenburg JL. 2011. Bacteroides in the infant gut consume milk oligosaccharides via mucus-utilization pathways. *Cell Host Microbe* 10:507–514. <https://doi.org/10.1016/j.chom.2011.10.007>
- Geerlings SY, Kostopoulos I, de Vos WM, Belzer C. 2018. Akkermansia muciniphila in the human gastrointestinal tract: when, where, and how? *Microorganisms* 6:75. <https://doi.org/10.3390/microorganisms6030075>

25. Ottman NA. 2015. Host immunostimulation and substrate utilization of the gut symbiont *Akkermansia muciniphila*. Wageningen University, Wageningen.
26. Kostopoulos I, Elzinga J, Ottman N, Klievink JT, Blijenberg B, Aalvink S, Boeren S, Mank M, Knol J, de Vos WM, Belzer C. 2020. *Akkermansia muciniphila* uses human milk oligosaccharides to thrive in the early life conditions *in vitro*. *Sci Rep* 10:14330. <https://doi.org/10.1038/s41598-020-71113-8>
27. Luna E, Parkar SG, Kirmiz N, Hartel S, Hearn E, Hossine M, Kurdian A, Mendoza C, Orr K, Padilla L, Ramirez K, Salcedo P, Serrano E, Choudhury B, Paulchakrabarti M, Parker CT, Huynh S, Cooper K, Flores GE, McBain AJ. 2022. Utilization efficiency of human milk oligosaccharides by human-associated *Akkermansia* is strain dependent. *Appl Environ Microbiol* 88. <https://doi.org/10.1128/AEM.01487-21>
28. Barcelo A, Claustre J, Moro F, Chayvialle JA, Cuber JC, Plaisancié P. 2000. Mucin secretion is modulated by luminal factors in the isolated vascularly perfused rat colon. *Gut* 46:218–224. <https://doi.org/10.1136/gut.46.2.218>
29. Aakko J, Kumar H, Rautava S, Wise A, Autran C, Bode L, Isolauri E, Salminen S. 2017. Human milk oligosaccharide categories define the microbiota composition in human colostrum. *Benef Microbes* 8:563–567. <https://doi.org/10.3920/BM2016.0185>
30. Korpela K, Salonen A, Hickman B, Kunz C, Sprenger N, Kukkonen K, Savilahti E, Kuitunen M, de Vos WM. 2018. Fucosylated oligosaccharides in mother's milk alleviate the effects of caesarean birth on infant gut microbiota. *Sci Rep* 8:13757. <https://doi.org/10.1038/s41598-018-32037-6>
31. Cani PD, de Vos WM. 2017. Next-generation beneficial microbes: the case of *Akkermansia muciniphila*. *Front Microbiol* 8:1765. <https://doi.org/10.3389/fmicb.2017.01765>
32. Shuoker B, Pichler MJ, Jin C, Sakanaka H, Wu H, Gascuña AM, Liu J, Nielsen TS, Holgersson J, Nordberg Karlsson E, Juge N, Meier S, Morth JP, Karlsson NG, Abou Hachem M. 2023. Sialidases and fucosidases of *Akkermansia muciniphila* are crucial for growth on mucin and nutrient sharing with mucus-associated gut bacteria. *Nat Commun* 14:1833. <https://doi.org/10.1038/s41467-023-37533-6>
33. Kosciw K, Deppenmeier U. 2020. Characterization of three novel β -galactosidases from *Akkermansia muciniphila* involved in mucin degradation. *Int J Biol Macromol* 149:331–340. <https://doi.org/10.1016/j.ijbiomac.2020.01.246>
34. Ndongo S, Armstrong N, Raoult D, Fournier P-E. 2022. Reclassification of eight *Akkermansia muciniphila* strains and description of *Akkermansia massiliensis* sp. nov. and *Candidatus Akkermansia timonensis*, isolated from human feces. *Sci Rep* 12:21747. <https://doi.org/10.1038/s41598-022-25873-0>
35. Kobayashi Y, Kawahara T, Inoue S, Kohda N. 2023. *Akkermansia biwaensis* sp. nov., an anaerobic mucin-degrading bacterium isolated from human faeces. *Int J Syst Evol Microbiol* 73. <https://doi.org/10.1099/ijsem.0.005697>
36. Guo X, Li S, Zhang J, Wu F, Li X, Wu D, Zhang M, Ou Z, Jie Z, Yan Q, Li P, Yi J, Peng Y. 2017. Genome sequencing of 39 *Akkermansia muciniphila* isolates reveals its population structure, genomic and functional diversity, and global distribution in mammalian gut microbiotas. *BMC Genomics* 18:800. <https://doi.org/10.1186/s12864-017-4195-3>
37. Kirmiz N, Galindo K, Cross KL, Luna E, Rhoades N, Podar M, Flores GE. 2020. Comparative genomics guides elucidation of vitamin B₁₂ biosynthesis in novel human-associated *Akkermansia* strains. *Appl Environ Microbiol* 86:e02117-19. <https://doi.org/10.1128/AEM.02117-19>
38. Becken B, Davey L, Middleton DR, Mueller KD, Sharma A, Holmes SC, Dallow E, Remick B, Barton GM, David LA, McCann JR, Armstrong SC, Malkus P, Valdivia RH. 2021. Genotypic and phenotypic diversity among human isolates of *Akkermansia muciniphila*. *mBio* 12:e00478-21. <https://doi.org/10.1128/mBio.00478-21>
39. van Passel MWJ, Kant R, Zoetendal EG, Plugge CM, Derrien M, Malfatti SA, Chain PSG, Woyke T, Palva A, de Vos WM, Smidt H, El-Sayed N. 2011. The genome of *Akkermansia muciniphila*, a dedicated intestinal mucin degrader, and its use in exploring intestinal metagenomes. *PLoS One* 6:e16876. <https://doi.org/10.1371/journal.pone.0016876>
40. Yin Y, Mao X, Yang J, Chen X, Mao F, Xu Y. 2012. dbCAN: a web resource for automated carbohydrate-active enzyme annotation. *Nucleic Acids Res* 40:W445–51. <https://doi.org/10.1093/nar/gks479>
41. Zhang H, Yohe T, Huang L, Entwistle S, Wu P, Yang Z, Busk PK, Xu Y, Yin Y. 2018. dbCAN2: a meta server for automated carbohydrate-active enzyme annotation. *Nucleic Acids Res* 46:W95–W101. <https://doi.org/10.1093/nar/gky418>
42. Finn RD, Clements J, Eddy SR. 2011. HMMER web server: interactive sequence similarity searching. *Nucleic Acids Res* 39:W29–37. <https://doi.org/10.1093/nar/gkr367>
43. Buchfink B, Xie C, Huson DH. 2015. Fast and sensitive protein alignment using DIAMOND. *Nat Methods* 12:59–60. <https://doi.org/10.1038/nmeth.3176>
44. Kumar S, Stecher G, Tamura K. 2016. MEGA7: molecular evolutionary genetics analysis version 7.0 for bigger datasets. *Mol Biol Evol* 33:1870–1874. <https://doi.org/10.1093/molbev/msw054>
45. Stecher G, Tamura K, Kumar S. 2020. Molecular evolutionary genetics analysis (MEGA) for macOS. *Mol Biol Evol* 37:1237–1239. <https://doi.org/10.1093/molbev/msz312>
46. Tamura K, Stecher G, Kumar S. 2021. MEGA11: molecular evolutionary genetics analysis version 11. *Mol Biol Evol* 38:3022–3027. <https://doi.org/10.1093/molbev/msab120>
47. Edgar RC. 2004. MUSCLE: multiple sequence alignment with high accuracy and high throughput. *Nucleic Acids Res* 32:1792–1797. <https://doi.org/10.1093/nar/gkh340>
48. Edgar RC. 2004. MUSCLE: a multiple sequence alignment method with reduced time and space complexity. *BMC Bioinformatics* 5:113. <https://doi.org/10.1186/1471-2105-5-113>
49. Sakurama H, Tsutsumi E, Ashida H, Katayama T, Yamamoto K, Kumagai H. 2012. Differences in the substrate specificities and active-site structures of two α -L-fucosidases (glycoside hydrolase family 29) from *Bacteroides thetaiotaomicron*. *Biosci Biotechnol Biochem* 76:1022–1024. <https://doi.org/10.1271/bbb.111004>
50. Shaikh FA, Lammerts van Bueren A, Davies GJ, Withers SG. 2013. Identifying the catalytic acid/base in GH29 α -L-fucosidase subfamilies. *Biochemistry* 52:5857–5864. <https://doi.org/10.1021/bi400183q>
51. Guillotin L, Lafite P, Daniellou R. 2014. Unraveling the substrate recognition mechanism and specificity of the unusual glycosyl hydrolase family 29 BT2192 from *Bacteroides thetaiotaomicron*. *Biochemistry* 53:1447–1455. <https://doi.org/10.1021/bi400951q>
52. Sela DA, Garrido D, Lerno L, Wu S, Tan K, Eom H-J, Joachimiak A, Lebrilla CB, Mills DA. 2012. *Bifidobacterium longum* subsp. infantis ATCC 15697 α -fucosidases are active on fucosylated human milk oligosaccharides. *Appl Environ Microbiol* 78:795–803. <https://doi.org/10.1128/AEM.06762-11>
53. Rodríguez-Díaz J, Monedero V, Yebra MJ. 2011. Utilization of natural fucosylated oligosaccharides by three novel α -L-fucosidases from a probiotic *Lactobacillus casei* strain. *Appl Environ Microbiol* 77:703–705. <https://doi.org/10.1128/AEM.01906-10>
54. Wu H, Rebello O, Crost EH, Owen CD, Walpole S, Bennati-Granier C, Ndeh D, Monaco S, Hicks T, Colville A, Urbanowicz PA, Walsh MA, Angulo J, Spencer DIR, Juge N. 2021. Fucosidases from the human gut symbiont *Ruminococcus gnavus*. *Cell Mol Life Sci* 78:675–693. <https://doi.org/10.1007/s00018-020-03514-x>
55. Fricker AD, Yao T, Lindemann SR, Flores GE. 2023. Interindividual diversity of human gut mucin-degrading microbial consortia. *BioRxiv*. <https://doi.org/10.1101/2023.05.13.540604>
56. van der Ark KCH, Aalvink S, Suarez-Diez M, Schaap PJ, de Vos WM, Belzer C. 2018. Model-driven design of a minimal medium for *Akkermansia muciniphila* confirms mucus adaptation. *Microb Biotechnol* 11:476–485. <https://doi.org/10.1111/1751-7915.13033>
57. Hardy MR, Townsend RR, Lee YC. 1988. Monosaccharide analysis of glycoconjugates by anion exchange chromatography with pulsed amperometric detection. *Anal Biochem* 170:54–62. [https://doi.org/10.1016/0003-2697\(88\)90089-9](https://doi.org/10.1016/0003-2697(88)90089-9)
58. Berry ASF, Farias Amorim C, Berry CL, Syrett CM, English ED, Beiting DP, Koshy AA. 2021. An open-source toolkit to expand bioinformatics training in infectious diseases. *mBio* 12:e0121421. <https://doi.org/10.1128/mBio.01214-21>
59. Bray NL, Pimentel H, Melsted P, Pachter L. 2016. Near-optimal probabilistic RNA-seq quantification. *Nat Biotechnol* 34:525–527. <https://doi.org/10.1038/nbt.3519>
60. Sonesson C, Love MI, Robinson MD. 2015. Differential analyses for RNA-seq: transcript-level estimates improve gene-level inferences. *F1000Res* 4:1521. <https://doi.org/10.12688/f1000research.7563.2>

61. Robinson MD, McCarthy DJ, Smyth GK. 2010. edgeR: a bioconductor package for differential expression analysis of digital gene expression data. *Bioinformatics* 26:139–140. <https://doi.org/10.1093/bioinformatics/btp616>
62. Robinson MD, Oshlack A. 2010. A scaling normalization method for differential expression analysis of RNA-seq data. *Genome Biol* 11:R25. <https://doi.org/10.1186/gb-2010-11-3-r25>
63. Ritchie ME, Phipson B, Wu D, Hu Y, Law CW, Shi W, Smyth GK. 2015. *limma* powers differential expression analyses for RNA-seq and microarray studies. *Nucleic Acids Res* 43:e47. <https://doi.org/10.1093/nar/gkv007>
64. McCarthy DJ, Smyth GK. 2009. Testing significance relative to a fold-change threshold is a TREAT. *Bioinformatics* 25:765–771. <https://doi.org/10.1093/bioinformatics/btp053>
65. Blighe K. 2018. EnhancedVolcano. Bioconductor.
66. Almagro Armenteros JJ, Tsirigos KD, Sønderby CK, Petersen TN, Winther O, Brunak S, von Heijne G, Nielsen H. 2019. SignalP 5.0 improves signal peptide predictions using deep neural networks. 4. *Nat Biotechnol* 37:420–423. <https://doi.org/10.1038/s41587-019-0036-z>
67. Davey LE, Malkus PN, Villa M, Dolat L, Holmes ZC, Letourneau J, Ansaldo E, David LA, Barton GM, Valdivia RH. 2023. A genetic system for *Akkermansia muciniphila* reveals a role for mucin foraging in gut colonization and host sterol biosynthesis gene expression. *Nat Microbiol* 8:1450–1467. <https://doi.org/10.1038/s41564-023-01407-w>
68. Derrien M, Vaughan EE, Plugge CM, de Vos WM. 2004. *Akkermansia muciniphila* gen. nov., sp. nov., a human intestinal mucin-degrading bacterium. *Int J Syst Evol Microbiol* 54:1469–1476. <https://doi.org/10.1099/ijs.0.02873-0>
69. Plovier H, Everard A, Druart C, Depommier C, Van Hul M, Geurts L, Chilloux J, Ottman N, Duparc T, Lichtenstein L, Myridakis A, Delzenne NM, Klievink J, Bhattacharjee A, van der Ark KCH, Aalvink S, Martinez LO, Dumas M-E, Maiter D, Loumaye A, Hermans MP, Thissen J-P, Belzer C, de Vos WM, Cani PD. 2017. A purified membrane protein from *Akkermansia muciniphila* or the pasteurized bacterium improves metabolism in obese and diabetic mice. *Nat Med* 23:107–113. <https://doi.org/10.1038/nm.4236>
70. Wu H, Owen CD, Juge N. 2023. Structure and function of microbial α -L-fucosidases: a mini review. *Essays Biochem* 67:399–414. <https://doi.org/10.1042/EBC20220158>
71. Summers EL, Moon CD, Atua R, Arcus VL. 2016. The structure of a glycoside hydrolase 29 family member from a rumen bacterium reveals unique, dual carbohydrate-binding domains. *Acta Crystallogr F Struct Biol Commun* 72:750–761. <https://doi.org/10.1107/S2053230X16014072>
72. Grootaert H, Van Landuyt L, Hulpiau P, Callewaert N. 2020. Functional exploration of the GH29 fucosidase family. *Glycobiology* 30:735–745. <https://doi.org/10.1093/glycob/cwaa023>
73. Huang K, Wang MM, Kulinich A, Yao HL, Ma HY, Martínez JER, Duan XC, Chen H, Cai ZP, Flitsch SL, Liu L, Voglmeir J. 2015. Biochemical characterisation of the neuraminidase pool of the human gut symbiont *Akkermansia muciniphila*. *Carbohydr Res* 415:60–65. <https://doi.org/10.1016/j.carres.2015.08.001>
74. Liu P, Zhang H, Wang Y, Chen X, Jin L, Xu L, Xiao M. 2020. Screening and characterization of an α -L-fucosidase from *Bacteroides fragilis* NCTC9343 for synthesis of fucosyl-N-acetylglucosamine disaccharides. *Appl Microbiol Biotechnol* 104:7827–7840. <https://doi.org/10.1007/s00253-020-10759-w>
75. Evans DF, Pye G, Bramley R, Clark AG, Dyson TJ, Hardcastle JD. 1988. Measurement of gastrointestinal pH profiles in normal ambulant human subjects. *Gut* 29:1035–1041. <https://doi.org/10.1136/gut.29.8.1035>
76. Mulualem DM, Agbavwe C, Ogilvie LA, Jones BV, Kilcoyne M, O'Byrne C, Boyd A. 2021. Metagenomic identification, purification and characterisation of the *Bifidobacterium adolescentis* BgaC β -galactosidase. *Appl Microbiol Biotechnol* 105:1063–1078. <https://doi.org/10.1007/s00253-020-11084-y>
77. Tailford LE, Money VA, Smith NL, Dumon C, Davies GJ, Gilbert HJ. 2007. Mannose foraging by *Bacteroides thetaiotaomicron*. *J Biol Chem* 282:11291–11299. <https://doi.org/10.1074/jbc.M610964200>
78. Guo B-S, Zheng F, Crouch L, Cai Z-P, Wang M, Bolam DN, Liu L, Voglmeir J. 2018. Cloning, purification and biochemical characterisation of a GH35 β -1,3/ β -1,6-galactosidase from the mucin-degrading gut bacterium *Akkermansia muciniphila*. *Glycoconj J* 35:255–263. <https://doi.org/10.1007/s10719-018-9824-9>
79. Kosciow K, Deppenmeier U. 2019. Characterization of a phospholipid - regulated β - galactosidase from *Akkermansia muciniphila* involved in mucin degradation. *Microbiologypopen* 8:e00796. <https://doi.org/10.1002/mbo3.796>
80. Robbe C, Capon C, Coddeville B, Michalski J-C. 2004. Structural diversity and specific distribution of O-glycans in normal human mucins along the intestinal tract. *Biochem J* 384:307–316. <https://doi.org/10.1042/BJ20040605>